Journal of Molecular Structure 1058 (2014) 298–307

Contents lists available at ScienceDirect

Journal of Molecular Structure

journal homepage: www.elsevier.com/locate/molstruc

Copper(II) complexes with cyanoguanidine and o-phenanthroline: Theoretical studies, *in vitro* antimicrobial activity and alkaline phosphatase inhibitory effect

Juan J. Martínez Medina [a], María S. Islas [b], Libertad L. López Tévez [a], Evelina G. Ferrer [b], Nora B. Okulik [a], Patricia A.M. Williams [b,*]

[a] Universidad Nacional del Chaco Austral, Cte. Fernández 755, (3700) Roque Sáenz Peña, Chaco, Argentina
[b] CEQUINOR, Dpto. de Química, Facultad de Ciencias Exactas 47 y 115 y Facultad de Ingeniería 1 y 47, Universidad Nacional de La Plata, (1900) Buenos Aires, Argentina

HIGHLIGHTS

- The calculated geometrical parameters are in agreement with the experimental values.
- The complexation increased: The antibacterial activity against *E. faecalis*. The post antibiotic and antifungal effects against *E. coli* and all fungal strains.
- The alkaline phosphatase inhibitor activities of the metal and cyanoguanidine.

GRAPHICAL ABSTRACT

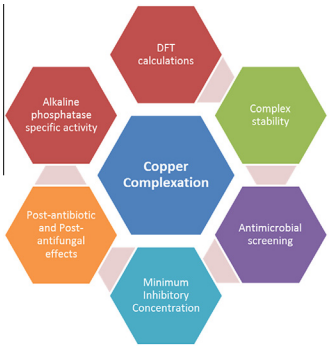

ARTICLE INFO

Article history:
Received 26 September 2013
Received in revised form 5 November 2013
Accepted 5 November 2013
Available online 15 November 2013

Keywords:
Phenanthroline
Cyanoguanidine
Copper complexes
DFT calculations
Antimicrobial properties
Alkaline phosphatase specific activity

ABSTRACT

Calculations based on density functional methods are carried out for two Cu(II) complexes with cyanoguanidine (cnge) and o-phenanthroline (o-phen): $[Cu(o\text{-}phen)_2(cnge)](NO_3)_2{\cdot}2H_2O$ (1) and $[Cu(o\text{-}phen)(cnge)(H_2O)(NO_3)_2]$ (2). The calculated geometrical parameters are in agreement with the experimental values. The results of Atoms in Molecules (AIM) topological analysis of the electron density indicate that the Cu–N(phen) bonds in complex (1) have lower electron density, suggesting that those bonds are stronger in complex (2). Moreover, the ionic character of the Cu–N bond in the complex (1) is slightly stronger than that in the complex (2) and this situation would explain the fact that only complex (2) was stable in water solution. For this reason, the antimicrobial and enzymatic assays were performed using complex (2). It is well known that the increased use of antibiotics has resulted in the development of resistant bacterial and fungal strains. In this context, the study of novel antimicrobial agents has an enormous importance and metal complexes represent an interesting alternative for the treatment of infectious diseases. The aim of this work is to prove the modification of some biological properties like antimicrobial activity or alkaline phosphatase inhibitory activity upon copper complexation.

The antimicrobial profile of the metal, the ligands and complex (2) was studied against several bacterial and fungal strains by different microbiological methods. The values of MIC indicate that the complexation increases the antibacterial activity against *Enterococcus faecalis*, but decreases this activity against *Pseudomonas aeruginosa*. The complex (2) exhibited longer PAEs/PAFEs than copper and o-phen against *Escherichia coli* and all fungal strains, and longer PAEs/PAFEs than some antibiotics or antifungal agents against *E. coli*, *Staphylococcus aureus* and *Candida albicans*. Complexation also improves the alkaline

* Corresponding author. Tel.: +54 (0)221 4240172; fax: +54 (0)221 4259485.
E-mail address: williams@quimica.unlp.edu.ar (P.A.M. Williams).

0022-2860/$ - see front matter
http://dx.doi.org/10.1016/j.molstruc.2013.11.014

phosphatase inhibitory effect of copper and cnge. Therefore, the interaction of copper(II) with N-containing ligands may provide a promising strategy for the development of novel drugs with enhanced antimicrobial activity or alkaline phosphatase inhibitory activity.

1. Introduction

Cyanoguanidine (cnge) has been recently recognized as nitrogenase substrate. The dimer functions as a dehydration coupling agent that links glucose and adenosine to phosphoric acid and then forms glucose-6-phosphate and adenosine-5′-phosphate, respectively [1]. Despite its biological importance, cnge also has commercial applications as intermediate in the formation of pharmaceuticals, pesticides, fungicides, and various polymers. Some transition metal ions (cf. copper, platinum and nickel) are able to catalyze the addition of alcohols to the nitrile group in cnge, forming n-alkylguanylureas that coordinates the metal ions [2–5].

In our previous paper [6], we report the molecular structure, bioavailability and bioactivity of two Cu(II) complexes with cnge and o-phenanthroline (o-phen), $[Cu(o\text{-phen})_2(cnge)](NO_3)_2{\cdot}2H_2O$ (1) and $[Cu(o\text{-phen})(cnge)(H_2O)(NO_3)_2]$ (2). The X-ray structure of the complex (1) reveals that the copper(II) ion is in a trigonal bipyramidal environment, coordinated to two o-phenanthroline groups acting as bidentate ligands through their N-atoms and to the cyanide N-atom of a cyanoguanidine molecule that enters coordination with a bent Cu–N–N angle. In the complex (2), the metal ion is at the center of a strongly elongated octahedral environment, equatorially coordinated to an o-phenanthroline ligand through its N-atoms, to the cyanide N-atom of a cyanoguanidine molecule that enters coordination radially and to a water molecule along the oxygen electron lone pair. The distorted octahedral coordination around copper is completed with two nitrate ions at the axial positions. As part of a continuing investigation on these complexes, in this paper we report calculations based on density functional theory (DFT), together with AIM analysis for the interactions between metal and the ligands. A charge density analysis will provide significant insight into the properties of the molecule as the total electron density distribution defines all the molecular properties in the ground state [7].

It is well known that copper is an essential trace element for many biological functions; however, in certain amounts copper can have toxic effects against microorganisms [8,9]. Besides, the antimicrobial action of o-phen has been demonstrated on several species of bacteria and fungus in some previous reports [10,11]. Moreover, the antimicrobial profile of some compounds can be modified upon complexation with copper ion and some copper complexes with antimicrobial activity have been studied [8,12–14]. Additionally, the increased use of antibiotics has resulted in the development of resistant strains. In this context, it is interesting to note the enormous importance of developing novel antimicrobial drugs for the treatment of infectious diseases [12,15]. In view of this, we have investigated the antimicrobial activity of copper, cnge, o-phen and complex (2) by agar diffusion and agar dilution methods for Gram-positive bacteria (*Staphylococcus aureus* and *Enterococcus faecalis*), Gram-negative bacteria (*Escherichia coli* and *Pseudomonas aeruginosa*) and fungus (*Candida parapsilosis* ATCC 22019, *Candida tropicalis* and *Candida albicans* of clinical isolates).

On the other hand, persistent suppression of bacterial growth following short antibiotic exposure has been well documented with a variety of microorganisms; this phenomenon is known as post-antibiotic effect (PAE) [16]. The PAE is the lag phase or recovery period of bacterial growth after brief exposure to an antibiotic. The PAE is a pharmacodynamic parameter and the presence of this effect may be an important consideration in designing antibiotic dosage regimens [17,18]. Determination of the PAE is recommended in pre-clinical evaluation of all new antimicrobial agents because it is a factor that influences optimal antimicrobial dosing intervals [19]. Also, the post-antifungal effect (PAFE) was previously defined as the time in which the antifungal agent was capable of causing growth suppression of the organism following limited exposure to the tested agents [20]. In the present study, the PAE for three strains of bacteria and the PAFE for three strains of fungi were studied. The PAEs/PAFEs were induced by exposure to twice the MIC ($2 \times$ MIC) of all compounds (metal, ligand and complex 2) for 1 h at 37 °C. The point at which microbial growth occurred was determined using a spectrophotometric method.

Alkaline phosphatase (ALP), as a group of ubiquitous enzymes, catalyzes the non-specific hydrolysis of phosphate monoester. ALP activity in serum is usually correlated with bone and liver diseases in vivo and is a marker of osteoblastic differentiation. The analysis of serum ALP has been extensively applied in routine clinic diagnosis [21]. It is demonstrated that some copper(II) complexes inhibits ALP activity [22,23]. The effect of the complex (2) on ALP activity has also been tested in order to determine a possible mechanism of the antimicrobial action of the compounds, by means of enzymatic inhibition.

2. Materials and methods

2.1. Reagents and instrumentation

All chemicals were of analytical grade. Copper(II) chloride dihydrate ($CuCl_2{\cdot}2H_2O$) was obtained from Merck, para-nitrophenyl phosphate (p-NPP), bovine intestinal ALP, solvents and all the other analytical grade chemicals used were purchased from Sigma. The growth media (Mueller Hinton Broth and Mueller Hinton Agar) and blank sterile discs were purchased from Brithania and Bioartis, respectively. $[Cu(o\text{-phen})(cnge)(H_2O)(NO_3)_2]$ complex was prepared according to the preparative technique described in our previous report [6]. Electronic absorption spectra were recorded on a spectrophotometer Agilent Technologies (Cary 60 UV–Vis).

2.2. Computational methodology

Calculations were performed using the GAUSSIAN 03 program package [24]. Molecular structures of ligands and metallic complexes were fully optimized at various levels. Geometry optimization procedures were started from the experimental crystallographic data employing the HF level with the 3-21G* basis set, and later, the effect of electron correlation on the molecular geometry was taken into account by using Becke's three-parameter hybrid, and the gradient corrected Lee–Yang–Parr correlational functional (B3LYP) [25] employing 6-31G(d,p) and 6-31+G(d,p) basis set.

Orthogonal rotations are commonly used for comparing macromolecular structures, and the root mean square deviation (RMSD) is a natural metric for quantitating the similarity of two optimally rotated structures [26]. To test the validity of quantum chemical calculations in reproducing the experimental structure of metal complexes RMSD between the coordinates of both macromolecules were calculated using Qmol package [27].

AIM topological analysis of electron density [28] has been elaborated using the PROAIM package [29] and the results have been evaluated in terms of electron density (ρ), density Laplacian ($\nabla^2\rho$):

$$\nabla^2\rho = \lambda_1 + \lambda_2 + \lambda_3$$

and bond ellipticity (ε):

$$\varepsilon = \lambda_1/\lambda_2 - 1$$

at bond critical points (BCP) where $\lambda_1 < \lambda_2 < 0 < \lambda_3$ are the eigenvalues of the Hessian of the BCP electron density. Calculated properties of electronic density at the BCP are labeled with the subscript 'b' throughout this work.

In AIM theory, atomic interactions are classified according to two limiting behaviors, namely, shared interactions and closed-shell interactions. Shared interactions are characteristic of covalent and polarized bonds and their main features are large values of ρ_b, $\nabla^2\rho_b < 0$ and $E_b < 0$, E_b being the local electronic energy density of the system calculated at the BCP and defined as the sum of the local kinetic energy density and the local potential energy density, both computed at the BCP. In contrast, closed-shell interactions, useful to describe ionic bonds, hydrogen bonds, and van der Waals interactions, are characterized by small values of ρ_b, $\nabla^2\rho_b > 0$ and $E_b > 0$.

2.3. Stability study of the dissolved complex

In our previous paper [6], we report that no appreciable changes occur in the position of very broad d–d bands upon dissolution of the complex (2) in water and conclude that there are not significant differences between the environment around the metal in the solid state and the solution. However, complex (1) may expand its coordination sphere upon dissolution, as suggested by the observed shift to the blue of the electronic band. Therefore, all microbiological and enzymatic determinations were carried out with the complex [Cu(o-phen)(cnge)(H_2O)(NO_3)$_2$] (2).

Moreover, in order to determine the stability of the complex (2) during the preparation of the solutions for the enzymatic and antimicrobial measurements, the variation of the electronic spectra with time was performed. Because of the low solubility of the complex (2) in water (at concentrations tested in agar dilution and diffusion methods), the dissolution has been carried out in 1/1 water/DMSO mixtures. Stability determinations were followed spectrophotometrically at least for 30 min that is the time of manipulation of the solid dissolved in the mixture during the ALP reaction or before its addition to the melted Mueller Hinton Agar (MHA) and transference to the square plate. For the analysis of PAE and PAFE, the complex (2) was dissolved in water at low concentrations and the stability determinations were followed spectrophotometrically at least for 120 min that is the time of manipulation of the solid dissolved in water before and during the exposure of the complex against the microorganism.

2.4. Antimicrobial assays

The antimicrobial profile of the metal ($CuCl_2{\cdot}2H_2O$), the ligands (cnge and o-phen) and the complex (2) have been studied against bacteria and fungi by two different microbiological methods (agar diffusion and agar dilution methods). Also, the PAE and PAFE were determined by a spectrophotometric method [17].

2.4.1. Bacterial and fungal strains

Control strains for the agar diffusion and agar dilution methods included: four strains of bacteria derived from the American Type Culture Collections (*E. coli* ATCC 35218, *P. aeruginosa* ATCC 27853, *S. aureus* ATCC 25923and *E. faecalis* ATCC 29212) and three strains of fungus (*C. parapsilosis* ATCC 22019, *C. tropicalis* and *C. albicans* of clinical isolates). The cultivation/assay medium for all strains was Mueller Hinton Broth or Agar (MHB, MHA) [30,31].

2.4.2. Preparation of inoculum

The inocula of bacterial and fungal strains were prepared from 18 h-old broth cultures. A McFarland 0.5 suspension was prepared for each isolate ($\sim 10^8$ colony forming units (CFU) per milliliter). Except for the agar dilution method with bacteria, in which a 1:10 dilution ($\sim 10^7$ CFU per mL) was made prior to inoculation, other assays were directly inoculated with this suspension [15,32–34].

2.4.3. Preparation of stock solutions

For the agar diffusion method, the metal and ligands were dissolved in water, whereas the complex (2) was dissolved in 50% aqueous dimethylsulfoxide (DMSO) to a final concentration of 100 mmol L^{-1}.

For the agar dilution method, the metal and ligands were dissolved in water, whereas the complex (2) was dissolved in 50% aqueous DMSO to a final concentration of 15 mg mL^{-1}. Serial twofold water dilutions were performed from the stock solutions of antimicrobial agents to give concentrations ranging from 14.65 to 15,000 μg mL^{-1}.

For the analysis of PAE and PAFE, the metal, the ligand o-phen and the complex (2) were dissolved in water. All solutions previously described were sterilized by filtration before use.

2.4.4. Agar diffusion method

As a preliminary screening, all compounds were tested against bacteria and fungi for their inhibitory activity using the disc diffusion method. A microbial suspension of turbidity equaled to 0.5 McFarland standard were uniformly spread using sterile cotton swabs on sterile Petri dishes containing MHA. Sterile filter paper discs of 6 mm in diameter were aseptically impregnated with 60 μL of the sterile solutions of each compound. The discs were allowed to stand until complete solvent evaporation and applied on the surface of previously inoculated solid agar. The plates were incubated aerobically at 37 °C for 18 and 48 h for bacteria and fungi, respectively. The diameters of inhibition zones were evaluated in millimeters. Values reported are an average of at least three independent experiments [15,35–37].

2.4.5. Agar dilution method

The minimum inhibitory concentration (MIC) of each compound against all strains of bacteria and fungi was determined by the agar dilution method. After preparation of serial twofold water dilutions of tested compounds, 0.5 mL of each dilution were added to 4.5 mL of melted MHA and poured into a square (45 × 15 mm) plate. The final concentrations ranging in the MHA were from 1.46 to 1500 μg mL^{-1}. An agar plate without antimicrobial agent and containing the same volume of DMSO was established as a sterility and organism growth controls. After cooling and drying, the agar surface was inoculated with 2 μL of the germ suspensions and incubated aerobically at 37 °C for 24 h and 48 h for bacteria and fungi, respectively. After incubation, MICs were interpreted and the inhibition of microbial growth was judged by comparison with growth in control plates. The MIC was defined as the lowest dilution of the complex that inhibited the visible growth of the test organism. A single colony or a faint haze caused by the inoculum was considered to be no growth. Each MIC experiment was repeated three times [15,33,34,38–43].

2.4.6. Analysis of PAE and PAFE by spectrophotometry

For PAE and PAFE testing, Eppendorfs containing 900 μL of broth with the antimicrobial compound at 2 × MIC were

inoculated with 100 μL of a germen suspension adjusted to 0.5 McFarland. Growth controls with inoculum but no antimicrobial compounds were included with each experiment. Inoculated Eppendorfs were placed in a thermostatic water bath at 37 °C for an exposure period of 1 h [18,20]. At the end of the exposure period the antimicrobial agent was removed by dilution [44,45]. The drug was inactivated by a 1:1000 dilution of the cultures in a pre warmed antimicrobial-free medium and reincubated at 37 °C [16,18]. The unexposed control cultures underwent the same "drug removal" procedures as the exposed cultures [44]. A 5% decrease in transmittance was used to define the point at which detection of growth occurred. The duration of PAE or PAFE was calculated by using the formula PAE/PAFE = T-C where T was the time required for a 5% decrease in transmittance for the antimicrobial-exposed organisms and C was the time required for the same inoculum in the control to decrease 5% in transmittance [17,18,20]. Transmittance readings (670 nm) were recorded at 5 min intervals [46]. Each PAE or PAFE measurement was carried out in duplicate [17,46].

2.5. Alkaline phosphatase specific activity

The effect of cooper, o-phen, cnge and the complex (2) on ALP activity was determined by UV–vis spectroscopy. The experimental conditions for ALP specific activity measurement were as follows: 1 μg/mL of bovine intestinal ALP and 5 mM of p-NPP were dissolved in the incubation buffer (pH = 10.5) and held for 10 min. The effects of the compounds were determined by addition of different concentrations (1–500 μM) of each one to the pre-incubated mixture. The solution of the complex was prepared in water/DMSO (50/50) before adding the buffer to obtain the desired final concentrations. The reaction was started by the addition of the substrate p-nitrophenyl phosphate (p-NPP) and the product p-nitrophenol was monitored by the absorbance changes at 405 nm. The effect of each concentration was tested at least in triplicate in three different experiments [22].

3. Results and discussion

3.1. DFT calculations

The geometries of the complexes were optimized without any constraints. The structures and atom labels of the complexes are depicted in Figs. 1 and 2.

The selected optimized geometric parameters for complexes 1 and 2 are gathered in Tables 1 and 2, respectively. The whole data for both complexes are listed in Supplementary material (Tables S1 and S2).

The DFT-optimized structure converged successfully to a structure, which is in well agreement with the experimental X-ray structure thus implying the adequacy of the theoretical method employed for the geometry optimizations of this particular system. The Cu–N(cnge) distances are in agreement with the experimental values and correlate with the shifts observed in the CN stretching bands in the FTIR experimental spectra of both complexes [6].

The general trends observed in the experimental data are well reproduced in the calculations. However, the comparison of the theoretical data with the experimental ones indicates that optimized angle values are slightly different with the experimental results. It should be noted that the geometry of the solid state structure is subjected to intra and intermolecular interactions, such as hydrogen bonding and van der Waals interactions, whereas the calculations are performed for isolated molecules.

The close structural relationship between the calculated and crystallographic observed structures is best illustrated with a

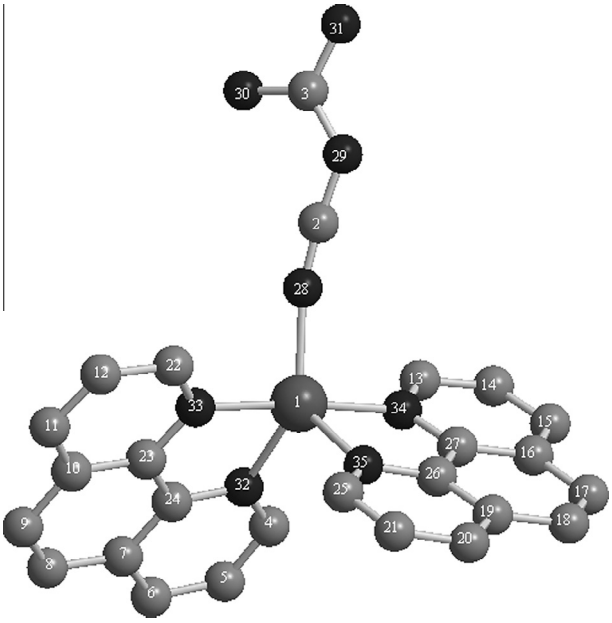

Fig. 1. Optimized geometry of $[Cu(o\text{-}phen)_2(cnge)](NO_3)_2{\cdot}2H_2O$ (1). Hydrogen atoms have been omitted for clarity, the black ball represents N atom and the gray ball represents C atom. Atom 1 is Cu.

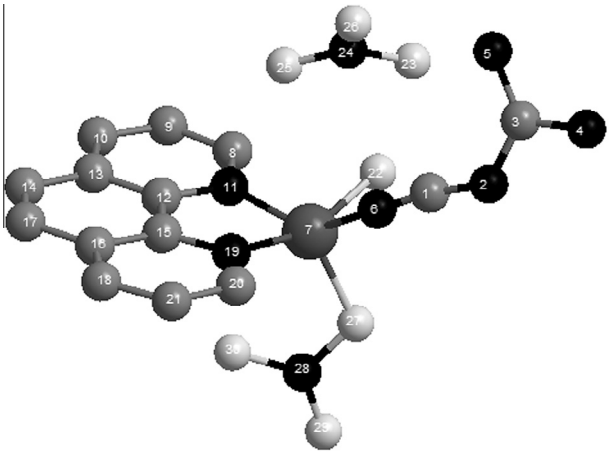

Fig. 2. Optimized geometry of $[Cu(o\text{-}phen)(cnge)(H_2O)(NO_3)_2]$ (2). Hydrogen atoms have been omitted for clarity, the black ball represents N atom, the white ball represent O atom and the gray ball represents C atom. Atom 7 is Cu.

RMS overlay error of 0.106 Å and 0.234 Å for complexes 1 and 2, respectively, when the atoms of the coordination sphere of copper are superimposed. The optimized structures of the isolated complexes are superimposed on the crystallographic structures in Fig. 3. The increased RMS overlay error of complex 2 is most probably due to solid state interactions as described above. The slightly higher value of RMS overlay error can be assigned to the fact that the X-ray structures were measured in a compacted crystalline form.

Details of the electron density topology at the CP can provide more insight into the nature of metal–ligand bonds. The results of AIM topological analysis of the electron density of complex (1) and complex (2) are collected in Tables 3 and 4, respectively. Topological analyses of the selected bonds of the isolated ligands are also shown for comparative propose.

The most important bonds to analyze within the AIM theory are obviously metal–ligands bonds. In particular, the attention is

Table 1
Selected bond lengths (Å) and angles (°) calculated for complex (1). Experimental values are reported for comparison purposes [6].

Bond lenghts[a]	Calc.[b]	Exptl.	Bond angles[a]	Calc.[b]	Exptl.
Cu1N28	2.0235	2.0045	N28Cu1N32	135.194	122.206
N28C2	1.1775	1.1465	N28Cu1N33	93.299	95.889
Cu1N34	2.0265	2.0015	N28Cu1N34	91.811	90.408
N34C13	1.3335	1.3215	N28Cu1N35	117.662	121.227
C13C14	1.4055	1.3985	N32Cu1N33	80.461	80.806
C25N35	1.3305	1.3265	N32Cu1N34	96.170	96.031
N35C26	1.3605	1.3525	N32Cu1N35	107.144	116.490
C26C27	1.4385	1.4265	N33Cu1N34	174.874	173.699
C26C19	1.4165	1.4015	N33Cu1N35	97.349	95.843
C27C16	1.4175	1.4075	N34Cu1N35	79.885	80.635
C27N34	1.3615	1.3505	C14C13N34	122.250	122.207
Cu1N35	2.1835	2.095	C12C22N33	122.097	122.007
Cu1N33	2.0265	1.9845	C7C24N32	123.026	122.979
Cu1N32	2.131	2.115	C23C24N32	117.282	117.236
C4N32	1.3315	1.3295	C21C25N35	122.839	121.717
N32C24	1.3615	1.3605	Cu1N28C2	167.366	154.004
C23N33	1.3605	1.3605	Cu1N32C4	130.791	131.911

[a] For the denomination of the atoms see Fig. 1.
[b] Calculated at B3LYP/6-31+g(d,p).

Table 2
Selected bond lengths (Å) and angles (°) calculated for complex (2). Experimental values are reported for comparison purposes [6].

Bond lenghts[a]	Calc.[b]	Exptl.	Bond angles[a]	Calc.[b]	Exptl.
C1–N2	1.289	1.292	N2C1N6	172.704	173.961
C1–N6	1.177	1.151	N2C3N4	114.796	123.357
N2–C3	1.335	1.345	C1N6Cu7	163.925	177.668
C3–N4	1.360	1.326	N6Cu7N11	140.800	93.045
C3–N5	1.336	1.317	N6Cu7N19	88.899	171.477
N6–Cu7	1.950	1.945	N6Cu7O34	87.741	92.409
Cu7–N11	1.944	1.990	N6Cu7O41	101.702	95.2
Cu7–N19	1.939	2.002	N11Cu7N19	83.787	82.584
Cu7–O34	1.971	1.966	N11Cu7O34	85.612	174.360
Cu7–O41	1.969	2.570	N11Cu7O41	116.683	87
C8–N11	1.337	1.324	N19Cu7O34	158.742	91.82
N11–C12	1.355	1.362	N19Cu7O41	112.573	77.3
C15–N19	1.359	1.357	O34Cu7O41	88.656	91.1
N19–C20	1.338	1.325	Cu7N11C8	129.050	130.139
O41–N42	1.389	1.251	Cu7N11C12	112.355	111.921
N42–O43	1.267	1.241	C8N11C12	118.544	117.928
O35–N38	1.350	1.251	Cu7N19C15	112.318	112.259
N38–O39	1.282	1.237	Cu7N19C20	129.040	129.403
N38–O40	1.314	1.241	Cu7O41N42	111.983	112.3

[a] For the denomination of the atoms see Fig. 2.
[b] Calculated at B3LYP/6-31+g(d,p).

focused on ρ_b and $\nabla^2\rho_b$, and their comparison with the reference values given by Trujillo and Bader to help in the characterization of a given bond [47]. All Cu–N BCP in both complexes display a

Table 3
Topological properties of selected bonds of the $[Cu(o\text{-phen})_2(cnge)](NO_3)_2{\cdot}2H_2O$ complex (1).[a,b]

Bond path	ρ_b	$\nabla^2\rho_b$	ε	E_b
Cu1–N28	0.0793	0.2753	0.02854	0.0688
Cu1–N32	0.0687	0.2066	0.0355	0.0517
Cu1–N33	0.0853	0.2629	0.0466	0.0658
Cu1–N34	0.0855	0.2615	0.0663	0.0653
Cu1–N35	0.0616	0.1936	0.0433	0.0484
C23–N33	0.3252	−0.9496	0.1144	−0.2373
	[0.3366]	[−1.1164]	[0.1009]	[−0.2791]
C23–C24	0.2986	−0.8083	0.1767	−0.2020
	[0.2857]	[−0.7462]	[0.1614]	[−0.1866]
N33–C22 38	0.3397	−0.8072	0.1129	−0.2018
	[0.3529]	[−0.9936]	[0.1289]	[−0.2482]
C10–C23	0.3048	−0.8191	0.1792	−0.2048
	[0.2993]	[−0.7841]	[0.1764]	[−0.1961]
C2–N28	0.4466	−0.1681	0.0146	−0.0420
	[0.4531)	[0.0226]	[0.0174]	[0.0056]
C2–N29	0.3699	−1.2101	0.0593	−0.3025
	[0.3470)	[−1.1947]	[0.0446]	[−0.2987]
C3–N29	0.3488	−1.2471	0.1575	−0.3117
	[0.3673)	[−1.321]	[0.2290]	[−0.3303]

[a] All quantities are in a.u.
[b] The values in square brackets are for the isolated ligands.

lower concentration of electronic charge with ρ_b ranging from 0.0936 to 0.1026 a.u. and positive values of $\nabla^2\rho_b$ (0.3482 a.u. and 0.3756 a.u., respectively). The energy densities, E_b, values at the BCP are positive in all cases indicating close-shell interactions. Same features shows Cu–O (water molecule) and Cu–O (nitrate ion) bonds.

The topological properties at critical points of the Cu–N bond are in good agreement with the corresponding values reported for Cu(II)–N donor ligand complex [ρ_b = 0.08–0.10 a.u., $\nabla^2\rho_b$ = 0.31–0.43 a.u., ε = 0.06] [48].

The C–C and C–N bonds correspond to covalent interactions, namely, a relatively large values for ρ_b and negative values for $\nabla^2\rho_b$. The ellipticities of bonds forming the phenanthroline rings have relatively large numerical values (c.a.: 0.1666 in C12–C15 bond), revealing their partial double bond character due electronic charge delocalization over the ring surface. These values are comparable to similar types of bonds found for other molecules [49–51]. The E_b values are negative as expected for covalent bonds. The topologic properties computed on C–C and C–N BCPs show very small changes with respect to their values in the isolated molecule of ligands.

We have previously reported that the complex (1) is unstable in water and the equilibrium is displaced towards complex (2), as suggested by the observed shift to the blue of the electronic band

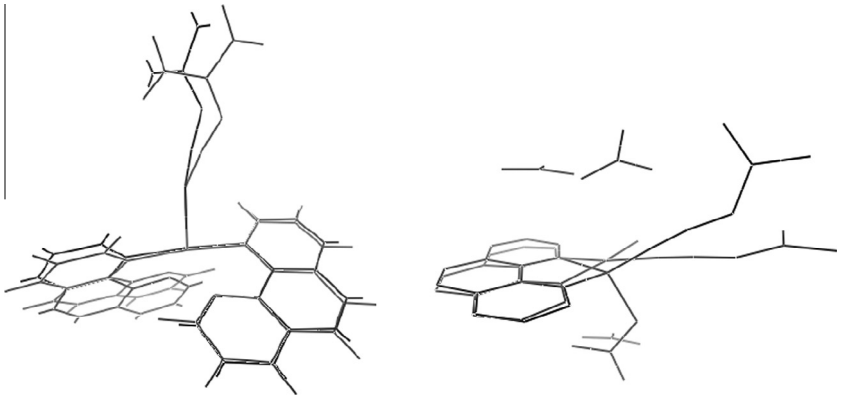

Fig. 3. Overlayed structures of the calculated (grey) and solid state (light grey) structures of 1 (left) and 2 (right).

Table 4
Topological properties of selected bonds of the [Cu(o-phen)(cnge)(H_2O)(NO_3)$_2$] complex (2).[a,b]

Bond path	ρ_b	$\nabla^2\rho_b$	ε	E_b
Cu7–N6	0.0936	0.3482	0.0423	0.0870
Cu7–O (water)	0.0828	0.3611	0.1054	0.0903
Cu7–O (nitrate)	0.0880	0.3818	0.0421	0.0954
Cu7–N11	0.1025	0.3661	0.0292	0.0915
Cu7–N19	0.1026	0.3756	0.0153	0.0939
C15–N19	0.3288	−1.0000	0.1035	−0.2500
	[0.3366]	[−1.1164]	[0.1009]	[−0.2791]
C12–C15	0.3087	−0.8686	0.1666	−0.2171
	[0.2857]	[−0.7462]	[0.1614]	[−0.1866]
N19–C20	0.3382	−0.8779	0.1133	−0.2195
	[0.3529]	[−0.9936]	[0.1289]	[−0.2482]
C12–C13	0.3109	−0.8517	0.1804	−0.2129
	[0.2993]	[−0.7841]	[0.1764]	[−0.1961]
C1–N6	0.4462	−0.1587	0.0188	−0.0397
	[0.4531)	[0.0226]	[0.0174]	[0.0056]
C1–N2	0.3674	−1.1508	0.0504	−0.2877
	[0.3470]	[−1.1947]	[0.0446]	[−0.2987]
C3–N2	0.3463	−1.2249	0.1614	−0.3062
	[0.3673)	[−1.3211]	[0.2290]	[−0.3303]

[a] All quantities are in a.u.
[b] The values in square brackets are for the isolated ligands.

[6]. The longer Cu1–N32 (o-phen) bond calculated and the experimental distances in complex (1) determined by X-ray measurements may be the cause of the instability of this ligand in aqueous solution. Moreover, the Cu–N(cnge) bond in complex (2) is slightly stronger than Cu–N(cnge) bond in complex (1), according to the calculated ρ_b and $\nabla^2\rho_b$ values (Tables 3 and 4). Also, the Cu–N(phen) bonds in complex (1) have lower electron density, suggesting that those bonds are stronger in complex (2). According to this trend, it is possible to affirm that the ionic character of the Cu–N bond in the complex (1) is slightly stronger than that in the complex (2). This situation would explain the different stability of both complexes.

3.2. Stability studies

In order to evaluate that in the *in vitro* studies the effects observed by the dissolved complex are due to the complex itself and not to its dissociation products, stability studies of complex (2) under the same antimicrobial experimental conditions were performed. This complex was dissolved in water and in a mixture of water/DMSO (50/50). The electronic visible spectra of the complex (2) are displayed in Figs. 4 and 5. It can be seen that the solutions remained stable for 3 h being the only species that contribute to the antimicrobial and enzymatic activities. In a previous work we have reported the stability of the ligands in aqueous solution [52].

3.3. Antimicrobial assays

It has previously been determined that complex (1) was not stable in water solution, being transformed in the $[CuAL]^+$ cation (A = o-phen, L = cnge) upon dissolution at physiological pH values [6]. For this reason, the antimicrobial assays were only performed using complex (2).

3.3.1. Agar diffusion method

As a first screening, all compounds were tested against bacteria and fungi using the discs diffusion method. Water/DMSO (50/50) mixture was used as negative control. Gentamicin and Ampicillin were used as positive reference standards for *E. coli*, *S. aureus* and *P. aeruginosa*, and *E. faecalis*, respectively. For all strains of Candida, Fluconazole was used as positive reference standard. Results of this

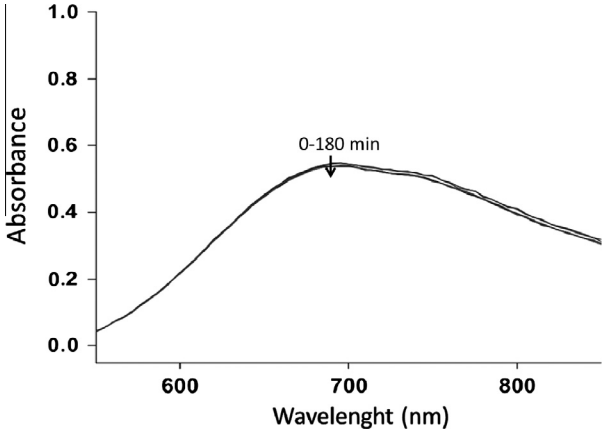

Fig. 4. Time variation of the electronic spectra of complex (2) in water (15 mmol L^{-1}).

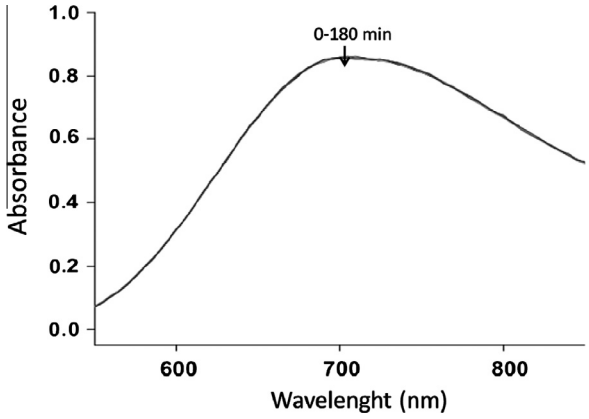

Fig. 5. Time variation of the electronic spectra of complex (2) in water/DMSO (20 mmol L^{-1}).

preliminary screening (Table 5) suggest antimicrobial activity of copper and o-phen against all bacterial and fungal strains at the tested concentrations. Our data indicate that the free ligand o-phen could exert a greater antimicrobial activity than copper. Taking into account the different measured inhibition zones, this ligand may have low values of minimum inhibitory concentration (MIC) against the strains of *Candida*, *S. aureus* and *E. coli*. The ligand cnge did not produce halos of inhibition at the tested concentrations, suggesting no antimicrobial activity of cnge. Our results also indicate that the complex (2) exerts antimicrobial activity against all tested strains (except *P. aeruginosa*). The observed order of zone of inhibition was *C. albicans* > *C. tropicalis* > *E. faecalis* > *E. coli*, *S. aureus* > *C. parapsilosis*.

3.3.2. Agar dilution method

The minimum inhibitory concentration (MIC) determinations of $CuCl_2.2H_2O$, o-phen and the complex (2) are displayed in Table 6. MIC values of Gentamicin and Ampicillin (positive reference standards) were determined against *E. coli*, *S. aureus* and *P. aeruginosa*, and *E. faecalis*, respectively. MIC values of Fluconazole (positive reference standard) were determined against all strains of Candida. *In vitro* measurements of antimicrobial activities with MIC values greater than 1000 μg mL^{-1} are considered with no relevance from a clinical perspective [53,54]. In this context, the antimicrobial activity of cnge against all tested strains (MIC > 1500) and the antibacterial activity of the ternary complex against *P. aeruginosa*

Table 5
Preliminary screening of antimicrobial profile of $CuCl_2{\cdot}2H_2O$, o-phen and the complex (2) against bacterial and fungal strains. Diameters of zones of inhibition in mm.

	Bacterial strains				Fungal strains		
	E. coli	*S. aureus*	*E. faecalis*	*P. aeruginosa*	*C. albicans*	*C. tropicalis*	*C. parapsilosis*
$CuCl_2{\cdot}2H_2O$	10.3 ± 0.6	11.3 ± 0.6	15.6 ± 0.6	9 ± 1.0	9 ± 1.0	12.3 ± 0.6	15 ± 1.0
o-phen	36 ± 1.0	40 ± 1.0	28.3 ± 0.6	19.6 ± 0.6	59.3 ± 1.1	43.3 ± 1.1	58.3 ± 1.5
Complex (2)	23 ± 1.0	23.6 ± 0.6	29 ± 1.0	0	43.3 ± 0.6	41 ± 1.0	14.3 ± 1.1
Gentamicin	23 ± 1.0	24.6 ± 0.6		24.6 ± 0.6			
Ampicillin			21 ± 1.0				
Fluconazole					43.6 ± 1.5	49 ± 1.0	39.6 ± 2.0

Table 6
Minimum inhibitory concentrations (MICs) of $CuCl_2$, o-phen and the complex (2) for bacterial and fungal strains. MIC values in $\mu g\ mL^{-1}$.

	Bacterial strains				Fungal strains		
	E. coli	*S. aureus*	*E. faecalis*	*P. aeruginosa*	*C. albicans*	*C. tropicalis*	*C. parapsilosis*
$CuCl_2{\cdot}2H_2O$	375	375	375	375	>1500	>1500	>1500
o-phen	12	24	94	375	3	12	12
Complex (2)	94	24	24	>1500	12	47	47
Gentamicin	0.8	0.2		1.5			
Ampicillin			0.4				
Fluconazole					>375	1.5	6

(MIC > 1500) are considered insignificant. These results are in concordance with the preliminary screening.

Copper is an essential element that functions as a cofactor during aerobic metabolism; however, in low or excessive amounts copper can have deleterious effects [9]. As expected [55], our data indicate that copper exerts moderate antibacterial effects toward the tested strains. Nevertheless, the antifungal activity of this metal is clinically irrelevant (MIC > 1500), in contraposition with the results expected by the preliminary screening. *C. albicans* and *C. tropicalis* have been previously described as a fungi higher resistant to elevated concentrations of copper [56,57]. Weissman et al. reported the isolation of two genes involved in copper detoxification in *C. albicans* (a copper-transporting P-type ATPase, CaCrp1 and a metallothionein, CaCup1). Both genes are induced by extracellular copper but CaCrp1 is more effective than CaCup1, because an extrusion pump functions catalytically, whereas a chelating agent (metallothionein) functions stoichiometrically [57]. Our data also indicate that the antimicrobial activity of this metal was enhanced by complexation. Some MIC values of copper(II) salts against different strains of bacteria and fungi have been previously reported in the literature including our previous report [55]. Patel et al. report MIC values of 460 $\mu g\ mL^{-1}$, 410 $\mu g\ mL^{-1}$ and 580 $\mu g\ mL^{-1}$ against *S. aureus*, *P. aeruginosa* and *E. coli*, respectively [58–60]. Recio Despaigne et al. report MIC values of >112 $\mu g\ mL^{-1}$, >214 $\mu g\ mL^{-1}$ and >285 $\mu g\ mL^{-1}$ against *S. aureus*, *P. aeruginosa* and *C. albicans*, respectively [12]. Chen et al. report a MIC of 256 $\mu g\ mL^{-1}$ against *S. aureus* [61]. Suksrichavalit et al. report that 32 $\mu g\ mL^{-1}$ of $CuCl_2{\cdot}2H_2O$ shows no activity against *C. albicans* [31]. These reports are in accordance with our results. Nevertheless, previously studies determine a MIC of >396 $\mu g\ mL^{-1}$ against *E. faecalis* ATCC19433 [12] and 64 $\mu g\ mL^{-1}$ against *C. albicans* ATCC 18804 [14] using the macro dilution test.

On the other hand, o-phen and its derivatives (including metal complexes) are of interest due to their potential activity against cancer, and viral, bacterial, and fungal infections [62]. The free ligand o-phen shows the lowest MIC values against *E. coli* and *S. aureus* [52,55] and against all strains of Candida, as expected by the results obtained on the preliminary screening. Some MIC values of o-phen against different bacterial and fungal strains were previously reported (MIC = 3.31 $\mu g\ mL^{-1}$ against *C. albicans* [63], MIC = 32 $\mu g\ mL^{-1}$ against *S. aureus* [64], MIC = 32 $\mu g\ mL^{-1}$, 256 $\mu g\ mL^{-1}$ and 128 $\mu g\ mL^{-1}$ against *S. aureus*, *P. aeruginosa* and *E. faecalis*, respectively [10]. Our data are in agreement with these reports. Nevertheless, Creaven et al. report MIC values of 51.34 $\mu g\ mL^{-1}$ and 99.11 $\mu g\ mL^{-1}$ against *S. aureus* and *E. coli* of clinical isolates, respectively [63]. Efthimiadou et al. report MIC values of 32 $\mu g\ mL^{-1}$ against *E. coli* and *P. aeruginosa* using broth dilutions method [64]. Roy et al. report a MIC of 25 $\mu g\ mL^{-1}$against *E. coli* JM109 [62]. Kalia et al. report MIC values of 32 $\mu g\ mL^{-1}$ against *E. coli* NCTC 10418 and *C. albicans* of clinical isolates [10]. The differences between the reported MIC values and our data could be attributed to the use of different microbial strains and different microbiological methods.

Currently, the antimicrobial properties of different copper complexes are being tested against numerous pathogens [8,12–14]. Our results indicate that the complexation is lower than the antibacterial activity of the metal and the ligand o-phen against *P. aeruginosa*. Moreover, the inhibitory activity of the complex (2) against all strains of Candida occurs at higher concentrations than o-phen. Interestingly, the inhibitory activity of the complex (2) against *E. faecalis* occurs at lower concentrations than copper(II) salt and o-phen.

In a previous paper we have demonstrated by fluorescence spectroscopy that the coordination of o-phen to Cd ($[Cd(o\text{-}phen)_2(SO_4)(H_2O)](cnge){\cdot}5H_2O$) increased the conformational rigidity of phenanthroline and that the delocalization of the ligand may be higher than in the chelate complex [65]. It is a well known fact that complexation increases the liposolubility of ionic metals [8,58]. In this study we have demonstrated by Atoms in Molecules analysis that the electronic density of phenanthroline diminishes by a ligand to metal charge transfer process having the complex more liposolubility and the cell permeability (Overtone's concept) may be higher [66] than the metal. It was previously shown that o-phen is a good antimicrobial agent. This ligand produces a synergic effect on the ternary complex through charge redistribution improving the activity of the metal and cnge in the ternary complex (in most of the tested strains).

For *E. Faecalis*, the passage of lipid-soluble materials through the membrane that surrounds the cell would be higher being more potent the antibacterial activity of the complex (a different mechanism will govern the other bacterial and fungal strains because of its different behavior with the compounds).

We have also investigated the antibacterial profile of $[Zn(phen)_2(cnge)(H_2O)](NO_3)_2{\cdot}H_2O$ complex [52]. In our previous

reports the antimicrobial measurements were performed using agar diffusion and agar dilution methods for cadmium [65] and zinc [52] complexes, respectively. The complex (2) and the cadmium complex show an improved activity against *E. faecalis*, whereas zinc complex shows less antibacterial activity than the ligands and the metal against this bacterial strain. The complex (2) and the zinc complex show less antibacterial activity than the ligands and the metal against *P. aeruginosa*, whereas cadmium complex shows an enhanced activity against this bacterial strain.

3.3.3. Analysis of PAE and PAFE by spectrophotometry

The PAE and PAFE are usually defined as the period of inhibition of bacterial or fungal growth after the antibiotic has been completely removed. This period can also be a measure of the delayed regrowth of bacteria/fungi after a short period of antibiotic/antifungal exposure [20,44]. A PAE or PAFE of 20 min or less were considered insignificant owing to the limitations of the testing procedure and were assigned a value of zero [17]. In this *in vitro* study, a spectrophotometric method was used to investigate the PAEs and PAFEs of the metal, the ligand and the complex (2) on strains of bacteria and fungi. The PAE and PAFE were induced by the exposure of the microorganism to twice the MIC of all compounds for 1 h at 37 °C. The PAEs of the metal and ligand o-phen on *P. aeruginosa* were not determined because the complex (2) exerts no activity against this bacterial strain (MIC > 1500). The ligand cnge against all strains and the metal against fungal strains exert no activity (MIC > 1500). The PAE or PAFE cannot be determined without MIC values. The values of PAEs and PAFEs are given in Table 7.

The experiment showed that 2 × MIC of copper caused measurable PAEs on the bacterial strains studied. The metal exhibited longer PAEs than the ligand o-phen in all cases. The observed order of PAEs of copper(II) chloride salt was *S. aureus* > *E. coli* > *E. faecalis*. Previously reported data [67] showed that the capacity of copper silicate to cause post antibiotic effect in *S. aureus* (ATCC 29213, at twice the MIC) of 2.1 h are in agreement with our present results.

The ligand o-phen exhibited a relevant PAE on *E. faecalis*. For the complex (2), the observed order of PAEs and PAFEs was *E. coli* > *S. aureus* > *E. faecalis* and *C. parapsilosis* > *C. albicans* > *C. tropicalis*, respectively. For *E. coli*, the complex exhibited longer PAEs than copper and o-phen. The complexation increases the PAE of the complex (2) against *E. coli*, but decreases the PAE against *E. faecalis*. For *S. aureus*, the complexation not modified the PAE. The enhanced PAE upon complexation for *E. coli* can be explained on the bases of Tweedy's chelation theory. On this theory, chelation reduces the polarity of the central metal atom because of partial sharing of its positive charge with the ligand. Further, it increases the delocalization of π-electrons over whole chelate ring and enhances lipophilicity of the complexes [8,58]. This increased lipophilicity of the complex (2) could be responsible for the longer PAE on Gram-negative bacteria (*E. coli*) because the complex could remain more time in the lipopolysaccharide and other lipidic components of the cell wall.

Table 7
Post-antibiotic effect (PAE) and post-antifungal effect (PAFE) of $CuCl_2{\cdot}2H_2O$, o-phen and the complex (2) at 2 × MIC for bacterial and fungal strains. PAE and PAFE values in h.

		$CuCl_2{\cdot}2H_2O$	o-phen	Complex (2)
Bacterial strains	*E. coli*	2.54 ± 0.04	0.54 ± 0.04	3.87 ± 0.04
	S. aureus	3.04 ± 0.21	0	3.04 ± 0.29
	E. faecalis	1.87 ± 0.04	1.58 ± 0.17	1.04 ± 0.12
Fungal strains	*C. albicans*	–	0	0.79 ± 0.04
	C. tropicalis	–	0	0.54 ± 0.04
	C. parapsilosis	–	0	5.46 ± 0.29

For the three fungal strains the complex exhibited longer PAEs than o-phen. The increased values of PAE on *E. coli* and PAFE on all fungal strains upon complexation are relevant in a clinical perspective because the presence of this effect may be an important consideration in designing antibiotic dosage regimens. A prolonged PAE should allow extension of antibiotic or antifungal dosing intervals beyond the time that antibiotic concentrations fall below the MIC [17]. Alovero et al. demonstrated that the PAE on *E. coli* (induced by an exposure of 10 times the MIC during 1 h) for the complex CIPX-Al was a bit longer than that of CIPX with values of 1.75 and 1.44 h, respectively [68]. Nevertheless, to our knowledge there are no PAE or PAFE reports for copper complexes.

The PAEs and PAFEs of the complex (2) were compared with the PAEs or PAFEs reported in the literature for antibiotic or antifungal agents (determined under similar experimental conditions against similar bacterial and fungal strains). The PAE of complex (2) on *E. coli* is longer than the PAE induced by Ampicillin [17,45], Ciprofloxacin [17,69,70], Tobramycin [17,71], Gentamicin [45,69], Garenoxacin [18], Enrofloxacin and Tetracycline [45], Chloramphenicol and Rifampicin [70]. The PAE of complex (2) on *S. aureus* is longer than the PAE induced by Gentamicin and Ciprofloxacin [69], Garenoxacin [18], Tobramycin [71], Ampicillin, Enrofloxacin [45]. This PAE is shorter than the PAE induced by Gentamicin (in contraposition with Domínguez et al. [69]) and Tetracycline [45], Daptomycin, Vancomycin and Nafcillin (against Methicillin-Susceptible and Methicillin-Resistant *S. aureus* Strains except MRSA-1) [72]. The PAE of complex (2) on *E. faecalis* is similar to that induced by Garenoxacin [18] and Penicillin G at 12xMIC against strain 4 [73]. This PAE is shorter than the PAE induced by Gentamicin at twice the MIC against all strains (except Strain 4) [73] and Penicillin G [72,73], Daptomycin and Vancomycin [72]. The PAFE of complex (2) on *C. albicans* is similar than Amphotericin B (1 × MIC) [74]. This PAFE is longer than 5-Fluorocytosine (1 × MIC) [74], Ketoconazole [74,75] and Fluconazole [74–76]. This PAFE is shorter than the PAFE induced by Amphotericin B [74–76] and 5-Fluorocytosine [74,75] at values higher than twice the MIC, MK-0991 and LY303366 [76], and Nystatin [75,77]. The PAFE of complex (2) on *C. tropicalis* is shorter than the PAFE induced by Nystatin (1xMIC) [77]. The PAFE of complex (2) on *C. parapsilosis* is shorter than the PAFE induced by Anidulafungin, Caspofungin and Micafungin [78], and Nystatin [77].

3.4. Alkaline phosphatase assays

Many microorganisms make enzymes in order to degrade complex substrates. The fact that the inorganic phosphate anion (Pi) cannot be synthesized by microbes makes alkaline phosphatases (ALPs) crucial for their survival. Cells must obtain phosphate from nucleic acids, phosphorylated sugars, proteins, etc., which hydrolysis provide Pi [79]. A diversity of phosphatases among different life forms is being discovered. Alkaline phosphatase monomers ranging from 15.5 kDa to 160 kDa have been reported for different strains. Some of them are trimeric and they also vary in their substrate specificities, pH ranges, and metal ion requirements. There is also diversity in the location of the enzymes being periplasmic in *E. coli*, membrane associated and extracellular in other strains [79]. Taking into account that we are studying enzymatic inhibition in bacteria and fungi herein, we have selected the ALP from bovine intestinal mucose for our inhibitory determinations. This ALP is a homodimeric metalloenzyme containing two zinc (Zn^{2+}) ions and one magnesium (Mg^{2+}) ion in each active site. When ALP catalyzed the hydrolysis of phosphomonoester, serine 102 coordinated to a zinc atom formed the phosphoseryl intermediate. This intermediate was hydrolyzed through nucleophilic attack by a water molecule activated by a second zinc atom [21].

The effect of the metal, the ligands and the complex (2) on ALP activity was evaluated (Fig. 6). As expected [22,23,55,80], the results show that the metal did not display significant inhibitory effect namely that copper(II) is not involved in the different mechanisms for enzymatic inhibitions (binding residues in proteins, coulombic or electrostatic interactions with the active site, inducement of protein aggregations or reversible inactivation due to a metal ion exchange). In addition, o-phen exerts strong inhibitory effect on ALP activity, cyanoguanidine behaves in a similar manner than the metal ion and complex (2) exerts inhibitory effects.

It has been determined that apo-bovine intestinal ALP, prepared using the ion-chelating agent EDTA exhibited a dramatic decrease of its hydrolase activity, concomitant to conformational changes in its quaternary structure and the total recovery of enzyme activity by divalent ion addition to the enzyme was not obtained using EDTA. This behavior is different using the enzyme from *E. coli*. In this case, the loss of the divalent ions induced protein monomerization and a total recovery of enzyme activity by divalent ion addition. Besides, the chelator o-phenanthroline also produced inhibition of the bovine intestinal enzyme. This effect was explained through a time dependent mechanism in which Zn^{2+}, which is required by ALP, is slowly removed, rendering the enzyme inactive. The effect was found to be reversible in discrepancy to the behavior of the more potent chelator EDTA [81].

A different mechanism of ALP inhibition was postulated for coordination complexes. In this case an interaction at the catalytic site of the enzyme was suggested as competitive inhibitors due to their binding at or near the active sites [23,80]. However, it was also proposed that the inhibitory effect on the activity of the enzymes that catalyze phosphoryl group transference can be attributed to a better bioavailability rather than to the increased potency at the phosphatase enzyme active sites caused by metal complexes [82].

In this work, we demonstrate that the complexation increases the inhibitory effect of the metal and the ligand cnge. The effect of o-phen on the enzymatic activity remains higher than that of the other compounds, as expected, due to the chelation effect exerted by the compound on the metallic sites of the enzyme, similar to the effect of EDTA.

In this context it can be seen that the antimicrobial effects of o-phen and the complex (2) could be due to their inhibition of the ALP enzyme and this interaction occurs by different mechanisms of action. In the copper(II) complex the higher interaction with the catalytic site because of the improvement of the bioavailability of copper(II) ion by complexation (higher liposolubility and cell permeability, see antimicrobial section) may be the causes of the inhibition of the enzymatic action. In the o-phen ligand the mechanism of the inhibiting power of the enzyme was different producing a chelation of the metals of the active site and rendering the apo-enzyme [80].

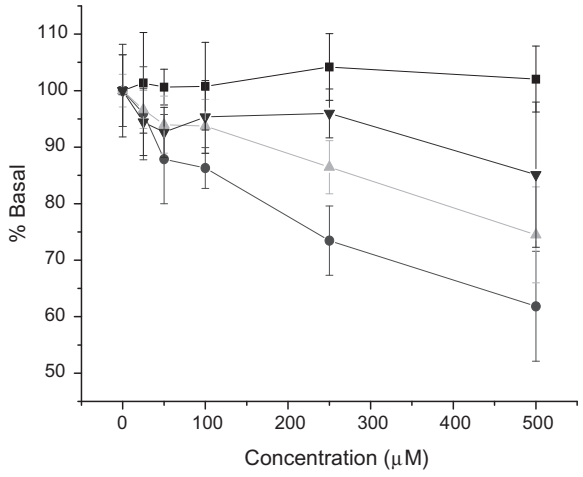

Fig. 6. Effect of $CuCl_2$ (Filled inverted triangle), o-phen (Filled circle), cnge (Filled square) and the complex 2 (Filled triangle, grey) on ALP activity from bovine intestinal mucose. Initial rate was determined by incubation of the enzyme at 37 °C for 10 min in the absence or presence of variable concentrations of the inhibitors. Basal activity was 5.2 ± 0.2 nmol pNP min^{-1} μg^{-1} protein.

4. Conclusions

The calculated geometrical parameters for the two Cu(II) complexes with cyanoguanidine (cnge) and o-phenanthroline (o-phen), $[Cu(o\text{-phen})_2(cnge)](NO_3)_2{\cdot}2H_2O$ (1) and $[Cu(o\text{-phen})(cnge)(H_2O)(NO_3)_2]$ (2) can be compared fairly well with the experimental values. The analysis of the interactions between metals and the ligands and an interpretation of the electronic structure of these complexes performed by the Atoms in Molecules analysis shows the nature of the main interactions between the metal and the ligand. The analysis of the topological properties calculated at the BCP shows that the character of the C–N and C–C bonds is covalent while the Cu–N chemical bonds have a closed-shell character. The topologic properties computed on C–C and C–N BCPs of cnge and o-phen are similar revealing that only very small changes are caused by the binding of ligand to metal to form the complex.

The stability study of the complex (2) in water or in the mixture water/DMSO indicates that the dissolved complex remained stable for 3 h being the only species that can contribute to the antimicrobial and enzymatic activities. On the other hand, complex (1) is unstable in water and the equilibrium is displaced towards the formation of complex (2). Therefore, we have undertaken the *in vitro* studies using only complex (2).

We have previously determined the inhibition of ALP activity by o-phenanthroline that uses a similar mechanism than EDTA. In this paper, we report that the complexation increases the antibacterial activity of the metal and the ligands against *E. faecalis*, but decreases their activity against *P. aeruginosa*. The complex (2) improves the alkaline phosphatase inhibitor activity of metal and cyanoguanidine and this may be one of the reasons of its higher antibacterial and antifungal activities (higher interaction with the active site of the enzyme because of its higher bioavailability than copper and cnge). Nevertheless, the MIC is an important antimicrobial assay to determine the susceptibility of some microorganisms against antimicrobial agents but provides limited information on the activity of the drug over time. In this context, the determination of PAE at 2 × MIC of all compounds was considered relevant to determine the modification of these pharmacodynamic parameter upon complexation. The complex (2) exhibited longer PAEs/PAFEs than copper and o-phen against *E. coli* and all fungal strains. Also, the complex (2) exhibited longer PAEs/PAFEs against *E. coli*, *S. aureus* and *C. albicans* than some antibiotics or antifungal agents. In this context, we can conclude that some biological properties are modified upon complexation with copper. Copper complexation may provide a promising strategy for the development of novel drugs with enhanced antimicrobial or alkaline phosphatase inhibitory activities.

Acknowledgments

This work was supported by UNLP, CICPBA, UNCAUS and CONICET. EGF and NBO are members of the Carrera del Investigador of CONICET. PAMW is a member of the Carrera del Investigador CICPBA, Argentina. MSI is a fellowship holder from CONICET.

Appendix A. Supplementary material

Supplementary data associated with this article can be found, in the online version, at http://dx.doi.org/10.1016/j.molstruc.2013.11.014.

References

[1] A.J. Belsky, T.B. Brill, J. Phys. Chem. A 102 (1998) 4509–4516.
[2] P. Ray, Chem. Rev. 61 (1960) 313–359.
[3] R.L. Dutta, A.M. Singh, J. Indian Chem. Soc. 52 (1975) 1000–1001.
[4] W.K. Baker Jr., M. Daniels, J. Inorg. Nucl. Chem. 25 (1963) 1194–1196.
[5] P.A.M. Williams, E.G. Ferrer, N. Baeza, O.E. Piro, E.E. Castellano, E.J. Baran, Z. Anorg. Allg. Chem. 631 (2005) 1502–1506.
[6] E.G. Ferrer, L.L. López Tévez, N. Baeza, M.J. Correa, N. Okulik, L. Lezama, T. Rojo, E.E. Castellano, O.E. Piro, P.A.M. Williams, J. Inorg. Biochem. 101 (2007) 741–749.
[7] P. Hohenberg, W. Kohn, Phys. Rev. 136 (1964) B864–B871.
[8] S. Chandraleka, K. Ramya, G. Chandramohan, D. Dhanasekaran, A. Priyadharshini, A. Panneerselvam, J. Saudi Chem. Soc. (2011), http://dx.doi.org/10.1016/j.jscs.2011.11.020.
[9] M. Ibrahim, F. Wang, M. Lou, G. Xie, B. Li, Z. Bo, G. Zhang, H. Liu, A. Wareth, J. Biosci. Bioeng. 112 (2011) 570–576.
[10] S.B. Kalia, G. Kaushal, M. Kumar, S.S. Cameotra, A. Sharma, M.L. Verma, S.S. Kanwar, Braz. J. Microbiol. 40 (2009) 916–922.
[11] M.O. Agwara, P.T. Ndifon, N.B. Ndosiri, A.G. Paboudam, D.M. Yufanyi, A. Mohamadou, B. Chem. Soc. Ethiopia 24 (2010) 383–389.
[12] A.A. Recio Despaigne, F.B. Da Costa, O.E. Piro, E.E. Castellano, S.R.W. Louro, H. Beraldo, Polyhedron 38 (2012) 285–290.
[13] C. Dendrinou-Samara, G. Psomas, C.P. Raptopoulou, D.P. Kessissoglou, J. Inorg. Biochem. 83 (2001) 7–16.
[14] I.C. Mendes, J.P. Moreira, A.S. Mangrich, S.P. Balena, B.L. Rodrigues, H. Beraldo, Polyhedron 26 (2007) 3263–3270.
[15] A. Berahou, A. Auhmani, N. Fdil, A. Benharref, M. Jana, C.A. Gadhi, J. Ethnopharmacol. 112 (2007) 426–429.
[16] M. Dolcino, A. Zoratti, E.A. Debbia, G.C. Schito, A. Marchese, Antimicrob. Agents Chemother. 46 (2002) 4022–4025.
[17] D.L. Rescott, D.E. Nix, P. Holden, J.J. Schentag, Antimicrob. Agents Chemother. 32 (1988) 450–453.
[18] G.A. Pankuch, M.R. Jacobs, P.C. Appelbaum, Antimicrob. Agents Chemother. 47 (2003) 1140–1142.
[19] W.J. Stubbings, J.M. Bostock, E. Ingham, I. Chopra, J. Antimicrob. Chemother. 54 (2004) 139–143.
[20] S. Taweechaisupapong, P. Ngaonee, P. Patsuk, W. Pitiphat, W. Khunkitti, S. Afr. J. Bot. 78 (2012) 37–43.
[21] M. Li, W. Ding, B. Baruah, D.C. Crans, R. Wang, J. Inorg. Biochem. 102 (2008) 1846–1853.
[22] N.M. Urquiza, S.G. Manca, M.A. Moyano, R. Arrieta Dellmans, L. Lezama, T. Rojo, L.G. Naso, P.A.M. Williams, E.G. Ferrer, Biometals 23 (2010) 255–264.
[23] C.J. Martin, W.J. Evans, J. Inorg. Biochem. 15 (1991) 177–178.
[24] M.J. Frisch, G.W. Trucks, H.B. Schlegel, P.M.W. Gill, B.G. Johnson, M.A. Robb, J.R. Cheeseman, T. Keith, G.A. Petersson, J.A. Montgomery, K. Raghavachari, M.A. Al-Laham, V.G. Zakrzewski, J.V. Ortiz, J.B. Foresman, J. Cioslowski, B.B. Stefanov, A. Nanayakkara, M. Challacombe, C.Y. Peng, P.Y. Ayala, W. Chen, M.W. Wong, J.L. Andres, E.S. Replogle, R. Gomperts, R.L. Martin, D.J. Fox, J.S. Binkley, D.J. Defrees, J. Baker, J.P. Stewart, M. Head-Gordon, C. Gonzalez, J.A. Pople, GAUSSIAN 03, Gaussian Inc., Pittsburgh, PA, 2003.
[25] A.D. Becke, J. Chem. Phys. 98 (1993) 5648–5652.
[26] D.R. Flower, J. Mol. Graphics Modell. 17 (1999) 238–244.
[27] J.D. Gans, D. Shalloway, J. Mol. Graphics Modell. 19 (2001) 557–559.
[28] R.F.W. Bader, Atoms in Molecules: A Quantum Theory, Clarendon Press, Oxford, 1990.
[29] F.W. Biegler-König, R.F.W. Bader, T.H. Tang, J. Comput. Chem. 3 (1982) 317–328.
[30] A. Klančnik, S. Piskernik, B. Jeršek, S.S. Možina, J. Microbiol. Methods 81 (2010) 121–126.
[31] T. Suksrichavalit, S. Prachayasittikul, C. Nantasenamat, C. Isarankura-Na-Ayudhya, V. Prachayasittikul, Eur. J. Med. Chem. 44 (2009) 3259–3265.
[32] F. Rowe, S. Vargas Superti, R. Machado Scheibe, C. Gomes Dias, Diagn. Micr. Infec. Dis. 43 (2002) 45–48.
[33] O. Koru, M. Ozyurt, Anaerobe 14 (2008) 161–165.
[34] C.E. Smith, B.E. Foleno, J.F. Barrett, M.B. Fresco, Diagn. Micr. Infec. Dis. 27 (1997) 85–92.
[35] M. Cavicchioli, A.C. Massabni, T.A. Heinrich, C.M. Costa-Neto, E.P. Abrão, B.A.L. Fonseca, E.E. Castellano, P.P. Corbi, W.R. Lustri, C.Q.F. Leite, J. Inorg. Biochem. 104 (2010) 533–540.
[36] M.K. Rauf, Imtiaz-ud-Din, A. Badshah, M. Gielen, M. Ebihara, D. de Vos, S. Ahmed, J. Inorg. Biochem. 103 (2009) 1135–1144.
[37] F. Shaheen, A. Badshah, M. Gielen, M. Dusek, K. Fejfarova, D. de Vos, B. Mirza, J. Organomet. Chem. 692 (2007) 3019–3026.
[38] G. Saravanan, V. Alagarsamy, C. Rajaram Prakash, J. Saudi Chem. Soc. (2011), http://dx.doi.org/10.1016/j.jscs.2011.12.010.
[39] G. Di Bonaventura, D. D'Antonio, G. Catamo, E. Ballone, R. Piccolomini, Int. J. Antimicrob. Agent 19 (2002) 147–154.
[40] G. Hall, A. Heimdahl, C.E. Nord, Anaerobe 4 (1998) 29–33.
[41] S. Weckesser, K. Engel, B. Simon-Haarhaus, A. Wittmer, K. Pelz, C.M. Schempp, Phytomedicine 14 (2007) 508–516.
[42] M.E. Arias, J.D. Gomez, N.M. Cudmani, M.A. Vattuone, M.I. Isla, Life Sci. 75 (2004) 191–202.
[43] M. Fang, J.H. Chen, X.L. Xu, P.H. Yang, H.F. Hildebrand, Int. J. Antimicrob. Agent 27 (2006) 513–517.
[44] P.C. Braga, M. Culici, M. Dal Sasso, Int. J. Antimicrob. Agent 24 (2004) 254–260.
[45] W. Fang, J. Microbiol. Methods 26 (1996) 151–159.
[46] M.S. Diarra, F. Malouin, M. Jacques, Int. J. Antimicrob. Agent 12 (1999) 229–237.
[47] J. Hernández-Trujillo, R.F.W. Bader, J. Phys. Chem. A 104 (2000) 1779–1794.
[48] M. Breza, P. Májek, Polyhedron 26 (2007) 4156–4160.
[49] E.A. Zhurova, C.F. Matta, N. Wu, V.V. Zhurov, A.A. Pinkerton, J. Am. Chem. Soc. 128 (2006) 8849–8861.
[50] E.J. Yearley, E.A. Zhurova, V.V. Zhurov, A.A. Pinkerton, J. Am. Chem. Soc. 129 (2007) 15013–15021.
[51] W.D. Arnold, L.K. Sanders, M.T. McMahon, A.V. Volkov, G. Wu, P. Coppens, S.R. Wilson, N. Godbout, E. Oldfield, J. Am. Chem. Soc. 122 (2000) 4708–4717.
[52] L.L. López Tévez, M.S. Islas, J.J. Martínez Medina, M. Diez, O.E. Piro, E.E. Castellano, E.G. Ferrer, P.A.M. Williams, J. Coord. Chem. 65 (2012) 2304–2318.
[53] J.C.A. Tanaka, C.C. da Silva, A.J.B. de Oliveira, C.V. Nakamura, B.P. Dias Filho, Braz. J. Med. Biol. Res. 39 (2006) 387–391.
[54] A.A. Aliero, A.D. Ibrahim, in: Y. Kumar (Ed.), Salmonella: A Diversified Superbug, In Tech, Open Access Company, Croatia, Europe, 2012, pp. 1–26 (Chapter 4).
[55] N.M. Urquiza, M. Soledad Islas, M.L. Dittler, M.A. Moyano, S.G. Manca, L. Lezama, T. Rojo, J.J. Martínez Medina, M. Diez, L.L. Tévez, P.A.M. Williams, E.G. Ferrer, Inorg. Chim. Acta 405 (2013) 243–251.
[56] A. Rehman, H. Farooq, A.R. Shakoori, Pak. J. Zool. 39 (2007) 405–412.
[57] Z. Weissman, I. Berdicevsky, B.Z. Cavari, D. Kornitzer, Proc. Natl. Acad. Sci. USA 97 (2000) 3520–3525.
[58] M.N. Patel, P.A. Dosi, B.S. Bhatt, V.R. Thakkar, Spectrochim. Acta Part A 78 (2011) 763–770.
[59] M.N. Patel, D.S. Gandhi, P.A. Parmar, Nucleos. Nucleot. Nucl. Acids 31 (2012) 445–460.
[60] M. Patel, D. Gandhi, P. Parmar, J. Coord. Chem. 64 (2011) 1276–1288.
[61] J.Y. Chen, X.X. Ren, Z.W. Mao, X.Y. Le, J. Coord. Chem. 65 (2012) 2182–2191.
[62] S. Roy, K.D. Hagen, P.U. Maheswari, M. Lutz, A.L. Spek, J. Reedijk, G.P. van Wezel, ChemMedChem. 3 (2008) 1427–1434.
[63] B.S. Creaven, D.A. Egan, D. Karcz, K. Kavanagh, M. McCann, M. Mahon, A. Noble, B. Thati, M. Walsh, J. Inorg. Biochem. 101 (2007) 1108–1119.
[64] E.K. Efthimiadou, M.E. Katsarou, A. Karaliota, G. Psomas, J. Inorg. Biochem. 102 (2008) 910–920.
[65] L.L. López Tévez, J.J. Martínez Medina, M.S. Islas, O.E. Piro, E.E. Castellano, L. Bruzzone, E.G. Ferrer, P.A.M. Williams, J. Coord. Chem. 64 (2011) 3560–3574.
[66] Y. Anjaneyulu, R.P. Rao, Synth. React. Inorg. Met. Org. Chem. 16 (1986) 257–272.
[67] J.G. Bartlett, T.J. Tan, T.V. Riley, Antimicrob. Agents Chemother. 51 (2007) 4505–4507.
[68] F.L. Alovero, M.E. Olivera, R.H. Manzo, Int. J. Antimicrob. Agent 21 (2003) 446–451.
[69] M.C. Domínguez, M. de la Rosa, M.V. Borobio, J. Antimicrob. Chemother. 47 (2001) 391–398.
[70] H.J. Wickens, R.J. Pinney, Int. J. Pharm. 227 (2001) 149–156.
[71] M. D'Arrigo, G. Ginestra, G. Mandalari, P.M. Furneri, G. Bisignano, Phytomedicine 17 (2010) 317–322.
[72] L.M. Bush, J.A. Boscia, M. Wendeler, P.G. Pitsakis, D. Kaye, Antimicrob. Agents Chemother. 33 (1989) 1198–1200.
[73] M.T. Hessen, P.G. Pitsakis, M.E. Levison, Antimicrob. Agents Chemother. 33 (1989) 608–611.
[74] M.T. García, M.T. Llorente, F. Mínguez, J. Prieto, J. Infect. 45 (2002) 263–267.
[75] A.N. Ellepola, L.P. Samaranayake, Oral Dis. 4 (1998) 260–267.
[76] E.J. Ernst, M.E. Klepser, M.A. Pfaller, Antimicrob. Agents Chemother. 44 (2000) 1108–1111.
[77] A.N. Ellepola, L.P. Samaranayake, J. Oral Pathol. Med. 28 (1999) 112–116.
[78] R.P. Smith, A. Baltch, L.H. Bopp, W.J. Ritz, P.P. Michelsen, Diagn. Micr. Infec. Dis. 71 (2011) 131–138.
[79] P. Prada, J.L. Curtze, J.E. Brenchley, Appl. Environ. Microbiol. 62 (1996) 3732–3738.
[80] C.J. Martin, J. Inorg. Biochem. 58 (1995) 89–107.
[81] M. Bortolato, F. Besson, B. Roux, Protein Struct. Funct. Genet. 37 (1999) 310–318.
[82] K.G. Peters, M.G. Davis, B.W. Howard, M. Pokross, V. Rastogi, C. Diven, K.D. Greis, E. Eby-Wilkens, M. Maier, A. Evdokimov, S. Soper, F. Genbauffe, J. Inorg. Biochem. 96 (2003) 321–330.